JOURNAL OF MATHEMATICAL PHYSICS VOLUME 45, NUMBER 6 JUNE 2004

Phase-space Green's functions for modeling time-harmonic scattering from smooth inhomogeneous objects

T. Melamed
Department of Electrical and Computer Engineering, Ben-Gurion University of the Negev, Beer Sheva 84105, Israel

(Received 7 January 2004; accepted 3 March 2004;
published online 10 May 2004)

The paper deals with inhomogeneous medium Green's functions in the phase-space domain by which the phase-space (local) spectral distributions of the field, scattered by a high contrast object due a genetic time-harmonic incidence, are evaluated. Two forms of phase-space Green's functions are considered: one that links induced sources in the configuration-space to phase-space distributions of the scattered field, while the other one directly links the phase-space distribution of the incident field to phase-space distributions of the scattered field. The scattering mechanism is described in terms of local samplings of the object function which are localized in the object domain according to the scattered- and incidence-processing parameters. Applications in the field of inverse scattering may be expected to yield fast and efficient algorithms, due to the capability of analytically evaluating (forward) scattering Green's functions. © *2004 American Institute of Physics.*
[DOI: 10.1063/1.1737812]

I. INTRODUCTION

The conventional spectral elements for wave synthesis are Green's functions or plane waves.[1] However, tracking these *global* basis functions in inhomogeneous environments or through interactions with objects is complicated, and the resulting representation integrals are spectrally distributed. Invoking constructive interference yields local observables in the form of ray fields, but in many situations a wider spectral range of basis functions is required.[2] Instead of using global basis functions that lead to distributed integrals, the representation may be localized *a priori* by using phase-space (PS) spectral representations in which the *local* basis wave-functions are beams. Each beam basis function then accounts for the radiation from a finite region in the source domain, thereby leading to compact spectral representations.

Several PS expansion schemes for wave propagation have been introduced. For *point source* configurations the source field can be expanded into an angular spectrum of beams that emanate from the source in all directions[3] (see also extension to the time-domain in Ref. 4). A different class of expansions applies for *extended source* configurations, utilizing a spectrum of shifted and tilted beams which emanate in all directions from all points in the source domain. Several alternative formulations for time-harmonic fields have been introduced:[5–11] In Refs. 8, 10, and 11, they have been placed within a unified PS format in which a PS distribution of beam propagators is *locally* matched to the source distribution. Recently, discrete PS spectral representations have been introduced, based on the discrete Wilson basis[12] and on frame theory.[13]

Inhomogeneous medium Green's functions are of fundamental significance for modeling wave propagation, inverse scattering, numerical methods, etc. Green's functions are wave objects that link sources in the configuration space, $\mathbf{r}'$, to the configuration observation domain, $\mathbf{r}$, by a convolution integral. These wave objects are global in nature in the sense that each point in the $\mathbf{r}'$ source domain contributes to *all* points in the $\mathbf{r}$-observation domain, hence, the difficulty in evaluating of these wave objects, both analytically and numerically. Since modeling wave propagation directly in the configuration-space implies global Green's functions, transferring the fields via phase-space (windowed-) Fourier transform facilitates the search after *localized Green's function*, which can be easily evaluated both asymptotically and numerically (see Ref. 3 and also

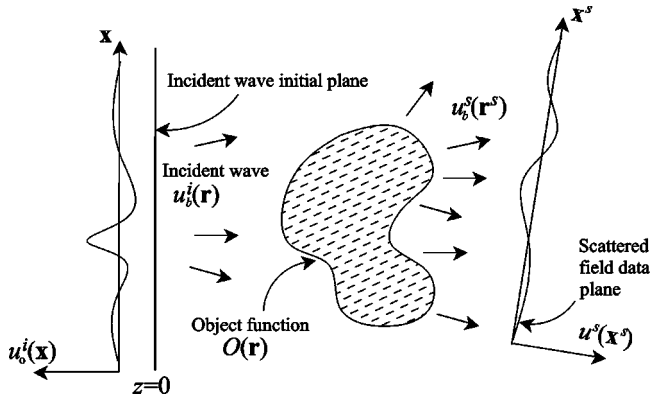

FIG. 1. Physical configuration; the object function $O(\mathbf{r})$ is illuminated by an incident wave $u_b^i(\mathbf{r})$ defined by its initial field distribution over the $z=0$ plane, whereas, the scattered field $u_b^s(\mathbf{r})$ is measured on a data plane $z^s=0$ between which the object is situated.

extension to the time-domain in Ref. 14). Furthermore, since wave interactions with scattering medium have been found to be local in nature, it is suggested that the evaluation of Green's functions should not be carried out in the configuration-space but rather in a *phase-space* (PS) transform domain, which extracts local radiation properties of the data and by that synthesizes local wave-medium interactions.[15,16] The above considerations have been applied in previous publications to the simple case of scattered field due to plane-wave incidence within the Born approximation.[15,16] The present contribution constitutes a general framework for the synthesis and analysis of *inhomogeneous* background scattering due to a *generic* incident wave with applications to inverse scattering, integral equation representation for propagation and scattering, and more.

Following this strategy, we are concerned with the field scattered by an object which is characterized by a wave velocity of $v(\mathbf{r})$, where $\mathbf{r}=(x_1,x_2,z)$ is the conventional Cartesian coordinate system, embedded in a homogeneous medium of save speed v_o (see Fig. 1). The total field $u(\mathbf{r})$, with a $e^{-i\omega t}$ time-dependence assumed and suppressed, satisfies the scalar Helmholtz equation

$$[\nabla^2+k^2(\mathbf{r})]\ \ u(\mathbf{r})=0,\ \ k(\mathbf{r})=\omega/v(\mathbf{r}), \tag{1}$$

subject to Sommerfeld radiation condition $\hat{\mathbf{r}}\cdot\nabla u(\mathbf{r})-iku(\mathbf{r})=o(r^{-1})$, for $r\to\infty$.

In the present investigation, the propagation of the field $u(\mathbf{r})$ in the inhomogeneous medium is formulated by the use of an inhomogeneous background $v_b(\mathbf{r})$ wave speed profile, and the deviation of the scattering medium $v(\mathbf{r})$ from the background $v_b(\mathbf{r})$ is described by the so-called *object function*

$$O(\mathbf{r})=v_o^2[v^{-2}(\mathbf{r})-v_b^{-2}(\mathbf{r})]. \tag{2}$$

The scattering object is illuminated by an incident field, $u_b^i(\mathbf{r})$, defined by the initial field distribution on $z=0$ plane $u_o^i(\mathbf{x})$. Note that $u_o^i(\mathbf{x})$ consists of incident (i.e., having sources in $z<0$ half space) field constituents only, and is therefore, independent of the background medium.

We are concerned with applying PS (local) spectrum techniques to the scattered field, therefore, the scattered field constituents shall be evaluated over planar apertures (observation planes), characterized by $z^s=0$, where $\mathbf{r}^s=(\mathbf{x}^s,z^s)$ with $\mathbf{x}^s=(x_1^s,x_2^s)$ are the Cartesian coordinate system associated with the observation plane (see Fig. 1). The scattered field over the observation plane, $u_b^s(\mathbf{x}^s)\equiv[u(\mathbf{r})-u_b^i(\mathbf{r})]|_{z^s=0}$, satisfies the Lipman–Schwinger integral equation

$$u_b^s(\mathbf{x}^s)=k_o^2\int d^3r'O(\mathbf{r}')u(\mathbf{r}')G_b(\mathbf{r}^s,\mathbf{r}')|_{z^s=0},\ k_o=\omega/v_o, \tag{3}$$

where $u=u_b^i+u_b^s$ is the total field propagating in v_b background medium, and G_b is the inhomogeneous *background* medium Green's function

$$[\nabla^2+k_b^2(\mathbf{r})]\,G_b(\mathbf{r},\mathbf{r}')=-\delta(\mathbf{r}-\mathbf{r}'),\quad k_b(\mathbf{r})=\omega/v_b(\mathbf{r}). \tag{4}$$

Here and henceforth, subscript b denotes background dependent constituents. Equation (3) describes the scattered field in terms of induced sources, $O(\mathbf{r}')u(\mathbf{r}')$, which are radiating in the perturbed medium $v_b(\mathbf{r})$. The background v_b-medium Green's function, $G_b(\mathbf{r},\mathbf{r}')$, propagates these induced sources to the aperture $z^s=0$ via the spatial convolution integral in (3). Relation (3) has been used for the so-called "Distorted Wave Born Approximation," in which the total field $u(\mathbf{r}')$ on the right-hand side of (3), is replaced by the incident field $u_b^i(\mathbf{r}')$ propagating in the background medium (see also discussion following (15)). This approximation is used for iteratively solving (forward) propagation and scattering problems, and for inverse scattering. In the following sections we will aim at obtaining *PS Green's functions* that link sources to scattered fields in a PS transform domain, rather than in the configuration-space.

II. CONFIGURATION-SPACE TO PHASE-SPACE GREEN'S FUNCTIONS

In order to obtain *PS Green's functions* that link sources to scattered PS field distributions, we shall project the scattered field distribution onto the PS (local) domain. In the next subsections, we shall define the (global) plane-wave spectrum and PS transform of the scattered field which are required for the formulation of the PS Green's function representation.

A. Space-wave-number (global) transforms

The wave number (plane-wave) spectrum, $\tilde{u}_o(\boldsymbol{\xi})$, of an initial field distribution, $u_o(\mathbf{x})$, on a planar surface is defined by the spatial Fourier transform

$$\tilde{u}_o(\boldsymbol{\xi})=\int_{-\infty}^{\infty} d^2x\;\; u_o(\mathbf{x})\exp(-ik_o\,\boldsymbol{\xi}\cdot\mathbf{x}), \tag{5a}$$

where, here and henceforth, plane-wave spectral distribution is denoted by superscript $\tilde{}$. In (5a), $\boldsymbol{\xi}=(\xi_1,\xi_2)$ is the normalized spatial wave number vector (with respect to $k_o=\omega/v_o$), and $\mathbf{x}=(x_1,x_2)$. Accordingly, the reconstruction of the initial field distribution is

$$u_o(\mathbf{x})=\left(\frac{k_o}{2\pi}\right)^2\int d^2\xi\;\; \tilde{u}_o(\boldsymbol{\xi})\;\; \exp(ik_o\,\boldsymbol{\xi}\cdot\mathbf{x}). \tag{5b}$$

The normalization with respect to the wave number k_o anticipates extension to the time-domain, rendering $\boldsymbol{\xi}$ frequency-independent, with direct geometrical interpretation in terms of the spectral plane-wave propagation angles. For the sake of simplicity, integration limits are omitted on all integrals extending from $-\infty$ to $+\infty$.

B. Phase-space processing of the scattered field

In this section, we summarize the PS analysis and synthesis formalisms that parameterize the scattered field on the initial plane $z^s=0$ (for further details refer to Ref. 11). For the desired *local* spectral analysis of the field distribution, we generate the *PS spectral distribution*, $U_b^s(\overline{\mathbf{X}}^s)$, via a windowed Fourier transform of the distribution in the configuration-space,

$$U_b^s(\overline{\mathbf{X}}^s)=\int d^2x^s\;\; u_b^s(\mathbf{x}^s)\;\; W^{s*}(\mathbf{x}^s;\overline{\mathbf{X}}^s),\quad W^s(\mathbf{x}^s;\overline{\mathbf{X}}^s)=w^s(\mathbf{x}^s-\overline{\mathbf{x}}^s)\exp[ik_o\overline{\boldsymbol{\xi}}^s\cdot(\mathbf{x}^s-\overline{\mathbf{x}}^s)], \tag{6}$$

where, here and henceforth, superscript s denotes scattered field constituents, the asterisk denotes the complex conjugate and $\overline{\mathbf{X}}^s=(\overline{\mathbf{x}}^s,\overline{\boldsymbol{\xi}}^s)$. Here, $w^s(\mathbf{x}^s)$ is a spatial window function, centered at $\mathbf{x}^s=(0,0)$. The vector $\overline{\mathbf{X}}^s$ incorporates the configuration-spectrum *PS coordinates* $(\overline{\mathbf{x}}^s,\overline{\boldsymbol{\xi}}^s)$, whence

$U_b^s(\overline{\mathbf{X}}^s)$ is referred to as a *PS distribution* of the initial field distribution $u_b^s(\mathbf{x}^s)$ over the $z^s=0$ plane. The transform in (6) extracts from $u_b^s(\mathbf{x}^s)$ the local spectrum around the $\overline{\boldsymbol{\xi}}^s$-directed propagation at the window center $\overline{\mathbf{x}}^s$. In typical propagation/scattering problems, the spectrum at a given $\overline{\mathbf{x}}^s$ is localized about a preferred spectral direction $\overline{\boldsymbol{\xi}}^s(\overline{\mathbf{x}}^s)$ that describes the (stationary) direction of propagation of the field at $\overline{\mathbf{x}}^s$ point (the so-called Lagrange manifold). Consequently, the PS spectrum $U^s(\overline{\mathbf{X}}^s)$ is localized *a priori* about the subdomain $(\overline{\mathbf{x}}^s,\overline{\boldsymbol{\xi}}^s)=(\overline{\mathbf{x}}^s,\overline{\boldsymbol{\xi}}^s(\overline{\mathbf{x}}^s))$ in the $\overline{\mathbf{X}}^s$-domain (see synthetic examples in Refs. 8, 11). Note that the PS spectrum of the scattered field depends on the specific background medium profile, $v_b(\mathbf{r})$, since according to (3), both the inhomogeneous medium Green's function, the medium object function, and the incident field propagating in the $v_b(\mathbf{r})$ medium, affect the scattered field.

The degree of spatial and spectral localization achieved by the PS transform can be quantified in terms of the spatial and spectral RMS widths of the window, defined, respectively, by

$$\Delta_{x^s}=\frac{1}{N^s}\left[\int d^2x^s|\mathbf{x}^s|^2 \quad |w^s(\mathbf{x}^s)|^2\right]^{1/2}, \tag{7a}$$

$$\Delta_{\xi^s}=\frac{k_o}{2\pi N^s}\left[\int d^2\xi^s|\boldsymbol{\xi}^s|^2 \quad |\tilde{w}^s(\boldsymbol{\xi}^s)|^2\right]^{1/2}, \tag{7b}$$

where $\tilde{w}^s(\boldsymbol{\xi}^s)$ is the plane-wave distribution (5a) of the window $w^s(\mathbf{x}^s)$, and

$$N^s=\left[\int d^2x^s|w^s(\mathbf{x}^s)|^2\right]^{1/2}=\frac{k_o}{2\pi}\left[\int d^2\xi^s|\tilde{w}^s(\boldsymbol{\xi}^s)|^2\right]^{1/2} \tag{8}$$

is the $\mathcal{L}^2_{\mathbf{x}^s}$ norm of w^s. Note that $\Delta_{x^s}\Delta_{\xi^s}\geqslant 1/k_o$ according to the uncertainty principle. The inverse PS transform is given by[11]

$$u_b^s(\mathbf{x}^s)=\left(\frac{k_o}{2\pi N^s}\right)^2\int d^4\overline{X}^s \quad U_b^s(\overline{\mathbf{X}}^s) \quad W^s(\mathbf{x}^s;\overline{\mathbf{X}}^s), \tag{9}$$

where W^s is given in (6). This representation has been used to obtain a PS field representation for homogeneous medium in the 2D (Refs. 8, 17) and 3D (Ref. 11) frequency- and time-domains.

C. PS Green's functions

In order to establish the locally-transformed Data–Object relation, we insert (3) into (6), obtaining

$$U_b^s(\overline{\mathbf{X}}^s)=k_o^2\int d^3r'O(\mathbf{r}')u(\mathbf{r}')B_b^s(\mathbf{r}';\overline{\mathbf{X}}^s), \tag{10}$$

with the scattering propagators

$$B_b^s(\mathbf{r}';\overline{\mathbf{X}}^s)=\int d^2x^s \quad W^{s*}(\mathbf{x}^s;\overline{\mathbf{X}}^s)G_b(\mathbf{r}^s;\mathbf{r}')\big|_{z^s=0}, \tag{11}$$

where $G_b(\mathbf{r},\mathbf{r}')$ is the background medium Green's function in (4) and $W^s(\mathbf{x}^s;\overline{\mathbf{X}}^s)$ is given in (6). Equation (10) describes the local spectrum of the data in terms of a spatial convolution integral of the induced sources $O(\mathbf{r}')u(\mathbf{r}')$ in the configuration-space, with $B_b^s(\mathbf{r}';\overline{\mathbf{X}}^s)$. Comparing relation (10) with the Lipman–Schwinger equation in (3), one finds that the two have essentially the same form. Therefore, $B_b^s(\mathbf{r}';\overline{\mathbf{X}}^s)$ may be regarded as *configuration-space to phase-space* (CS2PS) *Green's function* (see Appendix A for operator representation of the CS2PS Green's function). The CS2PS Green's function propagates the contribution of the configuration-space induced sources to

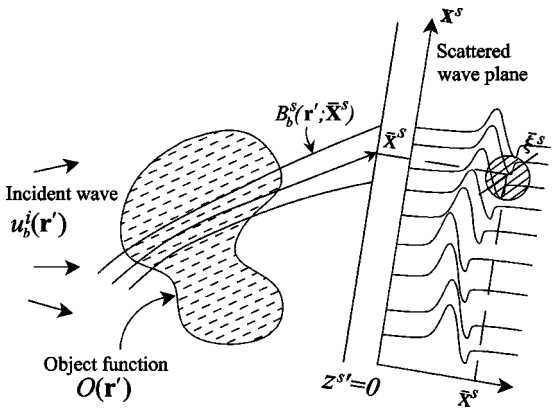

FIG. 2. Configuration-space to phase-space Green's function; the CS2PS Green's function is obtained by a spatial integration of the induced sources $u(\mathbf{r}')O(\mathbf{r}')$ multiplied by the scattering propagator, $B_b^s(\mathbf{r}';\overline{\mathbf{X}}^s)$. This results in a link between the total field propagating in the background medium, and a single phase-space constituent of the scattered field, $U_b^s(\overline{\mathbf{X}}^s)$. The integration domain is limited to points near the B_b^s beam-axis; thus, unlike the Lipman–Schwinger integral (3), the PS spectral distribution of the scattered field synthesizes wave interaction only near the beam-axis.

the PS transform of the data over the observation plane. Also, from (11), we note that the scattering propagators satisfy the wave equation in the v_b background medium, and therefore, for a proper choice of window function w^s, may be evaluated asymptotically using the method described in Sec. IV C (see also Fig. 2). Finally, using $u(\mathbf{r})=u_b^i(\mathbf{r})+u_b^s(\mathbf{r})$, we rewrite (10) in the form

$$U_b^s(\overline{\mathbf{X}}^s)=U_i^s(\overline{\mathbf{X}}^s)+U_s^s(\overline{\mathbf{X}}^s), \tag{12}$$

where

$$U_i^s(\overline{\mathbf{X}}^s)=k_o^2\int d^3r'\,O(\mathbf{r}')u_b^i(\mathbf{r}')B_b^s(\mathbf{r}';\overline{\mathbf{X}}^s), \tag{13}$$

and

$$U_s^s(\overline{\mathbf{X}}^s)=k_o^2\int d^3r'\,O(\mathbf{r}')u_b^s(\mathbf{r}')B_b^s(\mathbf{r}';\overline{\mathbf{X}}^s), \tag{14}$$

in which U_s^i and U_s^s are the contributions of the sources induced by either the incident or scattered fiels, respectively. The above exact formalism may be used for the Distorted Wave Born Approximation (DWBA) in which the total field $u(\mathbf{r}')$ in the exact formulation (3) is replaced by the incident field $u_b^i(\mathbf{r}')$ propagating in the background medium. The DWBA is often used for solving high contrast scattering iteratively, especially in inverse scattering scenarios. In the framework of the DWBA, we may use

$$U_b^s(\overline{\mathbf{X}}^s)\approx U_i^s(\overline{\mathbf{X}}^s). \tag{15}$$

The scattering propagators, $B_b^s(\mathbf{r}';\overline{\mathbf{X}}^s)$, result in a beam wave objects which, for the case of the Gaussian window in (23), are Gaussian beams localized about ray trajectories (i.e., beam-axes). Therefore, the CS2PS mapping in (10) (or (13)), is obtained by integrating over induced sources *locally about beam-axes*. The ray trajectories that describe the beam-axes depend on the background medium v_b and on the processing parameters: $\overline{\mathbf{x}}^s$ determines the emanating point of the ray from the data plane while $\overline{\boldsymbol{\xi}}^s$ sets its direction in the $\mathbf{r}'$ (source) domain (see Fig. 2).

The CS2PS representation in (10) or (12), has several advantages over the Lipman–Schwinger representation: (a) the inhomogeneous Green's function, $G_b(\mathbf{r},\mathbf{r}')$ is difficult to evaluate both analytically and numerically, while the scattering propagators may be evaluated asymptotically (see Sec. IV C); (b) the integration domain in (3) includes the entire object domain, since the induced sources, $O(\mathbf{r}')u(\mathbf{r}')$ exist in the entire object domain and contribute to each point $\mathbf{x}^s$ on the observation plane. Using the CS2PS relation, the integration domain is limited to points near the local Green's function (beam-) axis, since the beam exhibits Gaussian decay away from its axis (see (49) and Fig. 2). Though the induced sources exist in the entire object domain, the PS transform for a given set of PS variables, $\overline{\mathbf{X}}^s$, extracts from the scattered field only those constituents that are scattered in the direction $\overline{\boldsymbol{\xi}}^s$ and are aimed at the point $\overline{\mathbf{x}}^s$; and finally, (c) there exist applications in which the PS spectrum, rather than the scattered field, needs to be evaluated.[15,16] In such cases, direct evaluation using PS Green's function in (10) is more efficient than the conventional route of possibly solving (3), followed by PS processing via (6).

The CS2PS mapping in (10) exhibits *a priori* localization in the source domain only about the coordinates *transverse* to the beam-axis. Furthermore, the incident field $u_b^i(\mathbf{r})$, propagating in the inhomogeneous background medium, $v_b(\mathbf{r})$, has no closed form analytic expression. In the next section, we shall apply local processing to both *scattered* and *incident* fields, resulting in *a priori* localization in all three coordinates, as well as analytical (asymptotic) expressions for the local incident propagators and Green's functions.

III. PHASE-SPACE TO PHASE-SPACE GREEN'S FUNCTIONS

Following the strategy outlined in the previous section, we shall now consider applying PS processing to both *scattered* and *incident* fields. The PS transform operations over the scattered field have been introduced in Sec. II B. Next we define, in a similar way, the operations related to local processing of the incident field.

A. Local processing of the incident field

We generate the *incident field* PS spectral distribution in a way similar to (6), i.e.,

$$U^i(\overline{\mathbf{X}}^i)=\int d^2x \quad u_o^i(\mathbf{x}) \quad W^{i*}(\mathbf{x};\overline{\mathbf{X}}^i), \qquad W^i(\mathbf{x};\overline{\mathbf{X}}^i)=w^i(\mathbf{x}-\overline{\mathbf{x}}^i)\exp[ik_o\overline{\boldsymbol{\xi}}^i\cdot(\mathbf{x}-\overline{\mathbf{x}}^i)], \tag{16}$$

where, as in (6), $w^i(\mathbf{x})$ is a spatial window function. Here and henceforth, superscript i denotes *incident* field constituents and $\overline{\mathbf{X}}^i=(\overline{\mathbf{x}}^i,\overline{\boldsymbol{\xi}}^i)$ are the incidence *PS coordinates*. A key feature in (16) is that, unlike the scattered local spectrum, the incident one is *independent* of the propagation medium, $v_b(\mathbf{r})$. The window's properties (RMS widths, etc.) have been presented in Sec. II B (relations (7), (8)).

Using the inverse transform (as in (9) with $s\rightarrow i$), the PS superposition (16) of the initial field can be propagated into the region $z>0$, giving

$$u_b^i(\mathbf{r})=\left(\frac{k_o}{2\pi N^i}\right)^2\int d^4\overline{X}^i \quad U^i(\overline{\mathbf{X}}^i)B_b^i(\mathbf{r};\overline{\mathbf{X}}^i), \tag{17}$$

where N^i is the $\mathcal{L}_{\mathbf{x}}^2$ norm of w^i (similar to (8)), and the *PS incident propagator* B_b^i is the field radiated by each PS window element $W^i(\mathbf{x};\overline{\mathbf{X}}^i)$ in (9), and can therefore be expressed by Kirchhoff-type integration of the form

$$B_b^i(\mathbf{r};\overline{\mathbf{X}}^i)=\int 2W^i(\mathbf{x};\overline{\mathbf{X}}^i)\partial_{z'}G_b(\mathbf{r};\mathbf{r}')|_{z'=0}, \tag{18}$$

where $G_b(\mathbf{r};\mathbf{r}')$ is the v_b medium Green's function, and W^i is given in (16).

The representation in (17) describes the radiated field as a continuous superposition of shifted and tilted beams, centered at and directed along $\overline{\mathbf{x}}$ and $\overline{\boldsymbol{\xi}}$, respectively. The PS distribution $U^i(\overline{\mathbf{X}}^i)$ defines the excitation strengths of these beams via local matching to the aperture field $u_o^i(\mathbf{x})$.

B. PS Green's functions

By inserting the incident field PS representation in (17) into (13), and inverting the order of integration, one obtains

$$U_i^s(\overline{\mathbf{X}}^s)=\left(\frac{k_o^2}{2\pi N^i}\right)^2\int d^4\overline{X}^i \quad U^i(\overline{\mathbf{X}}^i)\int d^3r' O(\mathbf{r}')B_b^i(\mathbf{r}';\overline{\mathbf{X}}^i)B_b^s(\mathbf{r}';\overline{\mathbf{X}}^s). \tag{19}$$

Equation (19) links contributions of PS initial field distribution to the PS scattered field distribution over the $z^s=0$ observation plane in the following manner: the windowed incident (initial-) field distribution is propagated into the $\mathbf{r}'$ configuration-space via the local domain PS incident propagators $B_b^i(\mathbf{r}';\overline{\mathbf{X}}^i)$, which are beam-type wave objects. For a given $\overline{\mathbf{X}}^i$, the beam emanates from the processing-dependent point, $\overline{\mathbf{x}}^i$, in a processing-dependent direction, $\overline{\boldsymbol{\xi}}^i$, into $\mathbf{r}'$ space. The PS scattering propagators, $B_b^i(\mathbf{r}';\overline{\mathbf{X}}^i)$, accumulate, via d^3r' integration, contributions of the incident beams to the local scattered field PS distribution at point $\overline{\mathbf{x}}^s$ on the observation plane, arriving from direction $\overline{\boldsymbol{\xi}}^s$. The PS spectral distribution of the scattered field is obtained by collecting these contributions from all beams emanating from the incidence plane points, in all directions via the $d^4\overline{X}^i$ integration. The contribution of each incident-window element to the scattered PS spectrum is weighted by the PS distribution of the initial incident field.

In order to gain insight into the scattering mechanism, we rewrite (19) in the form

$$U_i^s(\overline{\mathbf{X}}^s)=k_o^2\int d^4\overline{X}^i \quad U^i(\overline{\mathbf{X}}^i)\Psi_b(\overline{\mathbf{X}}^s,\overline{\mathbf{X}}^i), \tag{20}$$

where

$$\Psi_b(\overline{\mathbf{X}}^s,\overline{\mathbf{X}}^i)=\int d^3r' O(\mathbf{r}')\Lambda_b(\mathbf{r}';\overline{\mathbf{X}}^i,\overline{\mathbf{X}}^s), \tag{21}$$

is hereby termed the *phase-space to phase-space* (PS2PS) *Green's function*, and $\Lambda_b(\mathbf{r}';\overline{\mathbf{X}}^i,\overline{\mathbf{X}}^s)$ is a sampling window in the $\mathbf{r}'$-object domain

$$\Lambda_b(\mathbf{r}';\overline{\mathbf{X}}^i,\overline{\mathbf{X}}^s)=\left(\frac{k_o}{2\pi N^i}\right)^2 B_b^i(\mathbf{r}';\overline{\mathbf{X}}^i)B_b^s(\mathbf{r}';\overline{\mathbf{X}}^s). \tag{22}$$

Relation (20) presents the PS spectrum of the time-harmonic scattered field distribution in terms of local spatial samples of $O(\mathbf{r})$ (Fig. 3). Since both $B_b^i(\mathbf{r}';\overline{\mathbf{X}}^i)$ and $B_b^s(\mathbf{r}';\overline{\mathbf{X}}^s)$ are beam-like wave objects, the multiplication in (22) results in a *local scattering cell* which exhibits a spatial Gaussian decay away from its center over the intersection of the incident and scattered beam-axes. Here, Λ_b provides windowing along the beam-axis as determined by the PS parameters $\overline{\mathbf{X}}^i$ and $\overline{\mathbf{X}}^s$. The above results imply that the interaction of the incident spectral beam with the object domain, when parameterized in terms of scattered Gaussian beam propagators (i.e., the scattered PS spectrum), occurs as if each scattered beam were *specularly reflected* from the local medium inhomogeneities (see Fig. 3 and further discussion following (56)).

IV. GAUSSIAN WINDOWS

In this section, we examine the special case of Gaussian windows, which have been used extensively for modeling beam propagation since they maximize the PS localization as implied by the uncertainty principle, and yield analytically trackable beam-type propagators.[3,8,14,11]

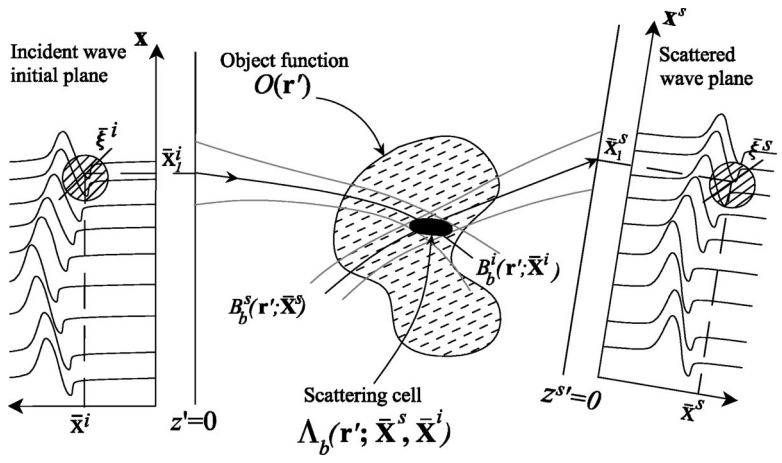

FIG. 3. Phase-space to phase-space mapping phenomenology; the phase-space transform, applied to both incident and scattered field distributions, synthesizes local reflections between isolated local cells, Λ_n, dynamically oriented and located according to the phase-space processing parameters $\bar{\mathbf{X}}^i$ and $\bar{\mathbf{X}}^s$. The PS2PS Green's function in (21) is obtained by a spatial windowing of the object function with the scattering cells.

A. Definitions

For locally (PS-)processing the scattered field distribution, we use a Gaussian window whose spatial and spectral distributions are

$$w^s(\mathbf{x}^s)=\exp\left[\frac{i}{2}k_o\mathbf{x}^s\quad\boldsymbol{\Gamma}^s\cdot\mathbf{x}^s\right],\quad \tilde{w}^s(\boldsymbol{\xi}^s)=\frac{2\pi i}{k_o\Gamma^s}\exp\left[-\frac{i}{2}k_o\boldsymbol{\xi}^s\quad(\boldsymbol{\Gamma}^s)^{-1}\cdot\boldsymbol{\xi}^s\right], \tag{23}$$

where $\boldsymbol{\Gamma}^s=\Gamma^s\mathbf{I}$, with $\mathbf{I}$ being the unity matrix and $\Gamma^s=\Gamma_r^s+i\Gamma_i^s$ is the window complex parameter with $\Gamma_i^s>0$. Anticipating extension to the time-domain, definition (23) has been constructed so that the frequency $k_o=\omega/v_o$ appears explicitly in the exponent, while Γ^s is *frequency-independent*. These features may be used to construct collimated time-domain wave objects. $\boldsymbol{\Gamma}^s$ is a complex symmetric matrix with $\mathrm{Im}\,\boldsymbol{\Gamma}^s$ positive definite, so that the quadratic phase in the exponent in (23), $\mathbf{x}^s\quad\boldsymbol{\Gamma}^s\cdot\mathbf{x}^s=[(x_1^{s2}+x_2^{s2})]\Gamma^s$, has a positive imaginary part that is generating a smooth Gaussian window which is strongest for $|\mathbf{x}^s|=0$ and weakens as $|\mathbf{x}^s|$ increases. The spatial and spectral localization can be quantified in terms of the spatial and spectral RMS widths of the windows given in (7), (8)

$$(N^s)^2=\pi/(k_o\Gamma_i^s),\quad \Delta_{x^s}=1/\sqrt{\Gamma_i^s k_o}=\Delta_{\xi^s}/|\Gamma^s|. \tag{24}$$

Note the uncertainty principle $\Delta_{x^s}\Delta_{\xi^s}=|\Gamma^s|/\Gamma_i^s k_o\geqslant 1/k_o$ with an equality for $\Gamma_r^s=0$.

Following the definition in (23), we shall define the *incident* field distribution processing window, $w^i(\mathbf{x})$, having the same structure as in (23), with the processing parameter Γ^i, i.e.,

$$w^i(\mathbf{x})=\exp\left[\frac{i}{2}k_o\mathbf{x}\quad\boldsymbol{\Gamma}^i\cdot\mathbf{x}\right],\quad \boldsymbol{\Gamma}^i=\Gamma^i\mathbf{I}, \tag{25}$$

etc. All the parametrization and analysis following (23) apply to w^i by replacing $\Gamma^s\to\Gamma^i$ and $\mathbf{x}^s\to\mathbf{x}$ in (23)–(24).

B. Special case: The Born approximation

In order to gain insight into the PS2PS mapping process, we first consider the Born approximation in which the background medium is the *homogeneous* medium v_o. In this case, the background Green's function is free-space Green's function, $G(\mathbf{r},\mathbf{r}')=\exp(ik_o|\mathbf{r}-\mathbf{r}'|)/(4\pi|\mathbf{r}$

$-\mathbf{r}'|$) and the PS propagators and scattering cells yield clear and simple asymptotic expressions. The general scattering over an inhomogeneous background is discussed in Sec. IV C.

1. Asymptotic evaluation of the scattering propagators

The formal integral representation of the scattering propagators using Gaussian windows may be obtained by inserting (23) into (11), with $G_b = G$ being free-space Green's function. Alternatively, a plane-wave spectral representation may be more useful for asymptotic evaluation. In order to obtain such a representation, we insert free-space Green's function plane-wave spectral representation[1]

$$G(\mathbf{r},\mathbf{r}') = \left(\frac{k_o}{2\pi}\right)^2 \int d^2\xi \frac{1}{-2ik_o\zeta} \exp[ik_o(\boldsymbol{\xi}\cdot(\mathbf{x}-\mathbf{x}') + \zeta|z-z'|)] \tag{26}$$

into (11) and invert the order of integration, yielding

$$B_b^s(\mathbf{r}^s;\overline{\mathbf{X}}^s) = \left(\frac{k_o}{2\pi}\right)^2 \int d^2\xi \frac{i}{2k_o\zeta} \tilde{w}^{s*}(\boldsymbol{\xi}-\overline{\boldsymbol{\xi}}^s) \exp[ik_o(-\boldsymbol{\xi}\cdot(\mathbf{x}^s-\overline{\mathbf{x}}^s) - \zeta z^s)], \tag{27}$$

where $\tilde{w}^s(\boldsymbol{\xi})$ is given in (23). For the Gaussian (scattering) window in (23), the scattering propagator has been evaluated asymptotically in Ref. 15 with connection to the PS processing of pulsed plane-wave excited scattering. It was found there that if the window is "large" on a wavelength scale, $B_b^s(\mathbf{r}^s;\overline{\mathbf{X}}^s)$ in (27) yields collimated beam fields in the $\mathbf{r}'$-domain. Via asymptotic evaluation and paraxial approximation, one obtains

$$B_b^s(\mathbf{r};\overline{\mathbf{X}}^s) = \frac{i}{2k_o\overline{\zeta}^s} \sqrt{\frac{\det\boldsymbol{\Gamma}^i(z_b^s)}{\det\boldsymbol{\Gamma}^s(0)}} \exp\left[ik_o\left(-z_b^s + \frac{1}{2}\mathbf{x}_b^s\boldsymbol{\Gamma}^s(z_b^s)\cdot\mathbf{x}_b^s\right)\right], \tag{28}$$

where

$$\boldsymbol{\Gamma}^s(z_b^s) = \begin{bmatrix} (-z_b^s - \overline{\zeta}^{s2}/\Gamma^{s*})^{-1} & 0 \\ 0 & (-z_b^s - 1/\Gamma^{s*})^{-1} \end{bmatrix}, \tag{29}$$

with $\overline{\zeta}^s = \sqrt{1-\overline{\boldsymbol{\xi}}^s\cdot\overline{\boldsymbol{\xi}}^s}$. In (28), we utilize the *beam-coordinates* $(x_{b_1}^s, x_{b_2}^s, z_b^s)$, defined, for a given PS point $\overline{\mathbf{X}}^s$, by the rotation transformation

$$\begin{bmatrix} x_{b_1}^s \\ x_{b_2}^s \\ z_b^s \end{bmatrix} = \begin{bmatrix} \cos\overline{\vartheta}^s\cos\overline{\varphi}^s & \cos\overline{\vartheta}^s\sin\overline{\varphi}^s & -\sin\overline{\vartheta}^s \\ -\sin\overline{\varphi}^s & \cos\overline{\varphi}^s & 0 \\ \sin\overline{\vartheta}^s\cos\overline{\varphi}^s, & \sin\overline{\vartheta}^s\sin\overline{\varphi}^s & \cos\overline{\vartheta}^s \end{bmatrix} \begin{bmatrix} x_1^s - \overline{x}_1^s \\ x_2^s - \overline{x}_2^s \\ z^s \end{bmatrix}, \tag{30}$$

where $(\overline{\vartheta}^s, \overline{\varphi}^s)$ are the spherical angles associated with the unit-vector (see Fig. 4)

$$\hat{\overline{\boldsymbol{\kappa}}}^s = (\overline{\boldsymbol{\xi}}^s, \overline{\zeta}^s) = (\sin\overline{\vartheta}^s\cos\overline{\varphi}^s, \sin\overline{\vartheta}^s\sin\overline{\varphi}^s, \cos\overline{\vartheta}^s). \tag{31}$$

Thus, the z_b^s axis coincides with the beam-axis in the positive (outward) $\hat{\overline{\boldsymbol{\kappa}}}^s$ direction; the transverse coordinates $\mathbf{x}_b^s = (x_{b_1}^s, x_{b_2}^s)$ are rotated such that $x_{b_2}^s$ is parallel to the z^s plane while $x_{b_1}^s$ lies in the plane $(\overline{\boldsymbol{\xi}}^s, \hat{\overline{\boldsymbol{\kappa}}}^s)$ with its positive direction defined so that $\overline{\boldsymbol{\xi}}^s\cdot\hat{\mathbf{x}}_{b_1}^s > 0$ (see Fig. 4). Furthermore, the system $(\mathbf{x}_b^s, z_b^s)$ is defined to be right-handed. Accordingly, the linear phase $\overline{\boldsymbol{\xi}}^s\cdot(\mathbf{x}^s-\overline{\mathbf{x}}^s)$ implied by the window function in the $z^s=0$ plane is operative in the $x_{b_1}^s$ direction *but not* in the $x_{b_2}^s$ direction. Consequently, $\overline{\boldsymbol{\xi}}^s$ affects only the $\boldsymbol{\Gamma}_{11}^s$ term in (29) but not the $\boldsymbol{\Gamma}_{22}^s$ term, thereby describing *astigmatic* beams.

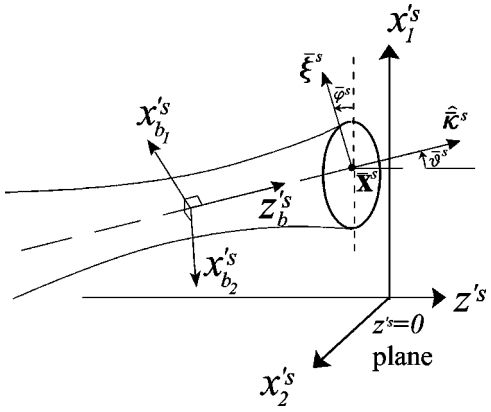

FIG. 4. Scattering propagators' local beam-coordinates; for a given PS spectral parameter $\bar{\mathbf{X}}^s$, the corresponding phase-space scattering propagator $B^s_b(\mathbf{r}';\bar{\mathbf{X}}^s)$ behaves like a collimated beam generated in the $\mathbf{r}'$-domain, whose axis reaches point $\bar{\mathbf{x}}^s$ on the $z'^s=0$ plane along the direction of the beam-axis unit-vector $\hat{\boldsymbol{\kappa}}^s$. The figure depicts the global fixed (x'^s_1,x'^s_2,z'^s) coordinate frame as well as the beam-centered coordinates $(x'^s_{b_1},x'^s_{b_2},z'^s_b)$ (referenced to the $z'^s=0$ plane), which extend along the beam-axis and along the two orthogonal directions perpendicular to the beam-axis.

The parameters of this astigmatic beam field, may be obtained by rewriting the diagonal elements in (29) in the form $\mathbf{\Gamma}=\mathrm{diag}(\Gamma_1,\Gamma_2)$ where $\Gamma^s_{1,2}(z^s_b)=(-z^s_b+Z^s_{1,2}-iF^s_{1,2})^{-1}$ with

$$Z^s_1=-\overline{\zeta}^{s^2}\Gamma^s_r/|\Gamma^s|^2,\quad Z^s_2=-\Gamma^s_r/|\Gamma^s|^2, \tag{32}$$

are identified as the beam *waist* location in the $(z^s_b,x^s_{b_{1,2}})$ plane, and

$$F^s_1=\overline{\zeta}^{s^2}\Gamma^s_i/|\Gamma^s|^2,\quad F^s_2=\Gamma^s_i/|\Gamma^s|^2, \tag{33}$$

are the corresponding *collimation lengths*. Furthermore, the *beam widths* in the $(z^s_b,x^s_{b_{1,2}})$ plane, $D^s_{1,2}$ are found from $\mathrm{Re}\,\Gamma^s(z^s_b)$, giving

$$D^s_{1,2}=\sqrt{F^s_{1,2}/k_o}\sqrt{1+(z^s_b-Z^s_{1,2})^2/F^{s2}_{1,2}}, \tag{34}$$

and the *phase front radius of curvature*, $R^s_{1,2}$ may be obtained from $\mathrm{Im}\,\Gamma^s(z^s_b)$, giving

$$R^s_{1,2}=(Z^s_{1,2}-z^s_b)+F^2_{1,2}/(Z^s_{1,2}-z^s_b). \tag{35}$$

The beam propagator astigmatism is caused by the beam tilt which reduces the effective initial beam width in the x_{b_1} direction. Note that the waist location Z, the collimation length F as well as the phase as a whole, are frequency-independent. However, beam width D is frequency dependent, being proportional to $k_o^{-1/2}$. These properties identify the scattering propagators as ''iso-diffracting'' wave packets.[18]

2. Asymptotic evaluation of the incident propagators

Using Gaussian windows, the PS incident propagators, $B^i_b(\mathbf{r};\bar{\mathbf{X}}^i)$ may be evaluated by inserting free-space Green's function into (18). In the present context it is convenient to express the free-space propagators by the plane-wave representation

$$B^i_b(\mathbf{r};\bar{\mathbf{X}}^i)=\left(\frac{k_o}{2\pi}\right)^2\int d^2\xi\ \ \tilde{w}(\boldsymbol{\xi}-\bar{\boldsymbol{\xi}}^i)\ \ \exp[ik_o(\boldsymbol{\xi}\cdot(\mathbf{x}-\bar{\mathbf{x}}^i)+\zeta z)]. \tag{36}$$

If w is wide on a wavelength scale then the spatial and spectral distributions of $\tilde{w}$ are localized around $\mathbf{x}=\overline{\mathbf{x}}^i$ and $\boldsymbol{\xi}=\overline{\boldsymbol{\xi}}^i$, respectively. Consequently, $B_b^i(\mathbf{r};\overline{\mathbf{X}}^i)$ behaves like a collimated beam whose axis emerges from the $z=0$ plane at $\mathbf{x}=\overline{\mathbf{x}}^i$ with a direction

$$\overline{\boldsymbol{\kappa}}^i=(\overline{\boldsymbol{\xi}}^i,\overline{\zeta}^i),\quad \overline{\zeta}^i=\sqrt{1-|\overline{\boldsymbol{\xi}}^i|^2}, \tag{37}$$

where $|\overline{\boldsymbol{\xi}}^i|^2=\overline{\boldsymbol{\xi}}^i\cdot\overline{\boldsymbol{\xi}}^i$. Next, the general formulation for the scattering process is evaluated for the special case of the Gaussian windows in (25). These windows enable closed form asymptotic evaluation of the PS2PS Green's function, $\Psi_b(\overline{\mathbf{X}}^s,\overline{\mathbf{X}}^i)$, and the scattering cell Λ_b. Via asymptotic evaluation and paraxial approximation, one obtains[11]

$$B_b^i(\mathbf{r};\overline{\mathbf{X}}^i)=\sqrt{\frac{\det\boldsymbol{\Gamma}^i(z_b^i)}{\det\boldsymbol{\Gamma}^i(0)}}\exp\left[ik_o\left(z_b^i+\frac{1}{2}\mathbf{x}_b^i\boldsymbol{\Gamma}^i(z_b^i)\cdot\mathbf{x}_b^i\right)\right], \tag{38}$$

where

$$\boldsymbol{\Gamma}^i(z_b^i)=\begin{bmatrix}(z_b^i+\overline{\zeta}^{i2}/\Gamma^i)^{-1} & 0\\ 0 & (z_b^i+1/\Gamma^i)^{-1}\end{bmatrix}, \tag{39}$$

with $\overline{\zeta}^i=\sqrt{1-\overline{\boldsymbol{\xi}}^i\cdot\overline{\boldsymbol{\xi}}^i}$. In (38), we utilize the beam-coordinates $(x_{b_1}^i,x_{b_2}^i,z_b^i)$ defined, for a given PS point $\overline{\mathbf{X}}^i$, by the transformation in (30) with $(\overline{\vartheta}^s,\overline{\varphi}^s)\to(\overline{\vartheta}^i,\overline{\varphi}^i)$ where $(\overline{\vartheta}^i,\overline{\varphi}^i)$ are the spherical angles associated with the unit-vector

$$\hat{\overline{\boldsymbol{\kappa}}}^i=(\overline{\boldsymbol{\xi}}^i,\overline{\zeta}^i)=(\sin\overline{\vartheta}^i\cos\overline{\varphi}^i,\sin\overline{\vartheta}^i\sin\overline{\varphi}^i,\cos\overline{\vartheta}^i). \tag{40}$$

The parametrization of the beam field in (38) may be obtained in a similar manner to (32)–(35).

The asymptotic beams in (38) facilitate insight into the role of the paraxial approximation: these beams do not satisfy the boundary condition $B^i(\mathbf{r};\overline{\mathbf{X}}^i)|_{z=0}=W^i(\mathbf{x};\overline{\mathbf{X}}^i)$, since near the $z=0$ plane, the paraxial approximation $z_b^i\gg\sqrt{x_{b_1}^{i\,2}+x_{b_2}^{i\,2}}$ is invalid. The paraxially approximated (astigmatic) beam is obtained by projecting the initial window onto the transverse plane $z_b^i=0$ over which the initial effective beam width in the $x_{b_1}^i$ direction is reduced by a factor of $\overline{\zeta}^i$ whereas the width in the $x_{b_2}^i$ direction remains unchanged. Therefore, the paraxial beam boundary conditions on a plane transverse to the beam propagation direction $(z_b^i=0)$ are

$$B^i(\mathbf{r}_b^i;\overline{\mathbf{X}}^i)|_{z_b^i=0}=\exp\left[\frac{i}{2}k_o\mathbf{x}_b^i\quad\boldsymbol{\Gamma}_{\text{parax}}^i\cdot\mathbf{x}_b^i\right], \tag{41}$$

with

$$\boldsymbol{\Gamma}_{\text{parax}}^i=\begin{bmatrix}\Gamma^i/\overline{\zeta}^{i2} & 0\\ 0 & \Gamma^i\end{bmatrix}. \tag{42}$$

Comparing the scattering propagator in (28) to the incident propagator in (38), one finds that they have a similar Gaussian beam type form. They differ mainly in the beam-axis directions: in (40) the beam-axis is directed along the *outgoing* direction (i.e., towards the scattering object) whereas in (31), the scattering propagators are directed *away from the object*. Furthermore, the incident beam is forward propagating (i.e., accumulates positive phase along the beam-axis), whereas the $-z_b^s$ term in (29) implies that the scattering propagators are *back-propagated* into the scattering object domain.

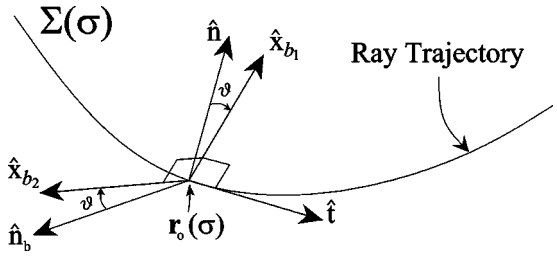

FIG. 5. Local beam-coordinates and ray trajectories; the beam propagator is propagating along ray trajectory Σ. The local orthogonal coordinate system $\mathbf{r}=\mathbf{r}_o(\sigma)+x_1\hat{\mathbf{x}}_1+x_2\hat{\mathbf{x}}_2$, where σ is the arc length along the ray trajectory, is obtained by the rotation transformation in (45).

3. PS2PS mapping

Next, we examine the local scattering cell in the $\mathbf{r}'$ object domain, $\Lambda_b(\mathbf{r}';\overline{\mathbf{X}})$, under the Born approximation. By inserting (38) with (28) into (22), one obtains

$$\Lambda_b(\mathbf{r}';\overline{\mathbf{X}}^i,\overline{\mathbf{X}}^s)=\frac{ik_o^3}{8\overline{\zeta}^s(\pi N^i)^2}\sqrt{\frac{\det\boldsymbol{\Gamma}^i(z_b^i)}{\det\boldsymbol{\Gamma}^i(0)}}\sqrt{\frac{\det\boldsymbol{\Gamma}^s(z_b^s)}{\det\boldsymbol{\Gamma}^s(0)}}$$
$$\times\exp\left[ik_o\left(z_b^i-z_b^s+\frac{1}{2}\mathbf{x}_b^i\boldsymbol{\Gamma}^i(z_b^i)\cdot\mathbf{x}_b^i+\frac{1}{2}\mathbf{x}_b^s\boldsymbol{\Gamma}^s(z_b^s)\cdot\mathbf{x}_b^s\right)\right]. \tag{43}$$

Relation (43) describes a local 3D spatial window; it is centered at the intersection of the incident and scattering propagators axes, where both $\mathbf{x}_b^i$ and $\mathbf{x}_b^s$ are zero, and exhibits a Gaussian decay as the transverse coordinates $\mathbf{x}_b^i$ and $\mathbf{x}_b^s$ increase. The orientation of the cell is determined by the rotation transformation in (30) for incident and scattering propagators, and by the processing parameters Γ^i and Γ^s. For the special case $\Gamma^i=\Gamma^s$, the exponent in (43) contains the sum of $\mathbf{x}_b^i$ and $\mathbf{x}_b^s$. Since both are determined by a rotation transformation of the (30) kind, the result is a new rotation transformation that bisects the incident direction $\hat{\boldsymbol{\kappa}}^i$ in (37) with the scattering direction $\hat{\boldsymbol{\kappa}}^s$ in (31). Therefore, the interaction of the incident spectral beam with the object domain, when parameterized in terms of scattered Gaussian beam propagators, occurs as if each scattered beam were *specularly reflected* from the local medium inhomogeneities (see Fig. 3 and further discussion following (56)).

C. Propagation in the perturbed medium

Next, we consider the propagation of beam propagators (such as B_b^i and B_b^s) in an *inhomogeneous medium* with a wave velocity $v_b(\mathbf{r})$.

1. Local beam-coordinates

An asymptotic solution for general beam-type propagation in an inhomogeneous medium is given in Ref. 3 (see also extension to the time-domain in Refs. 14 and 19). It has been shown there that the field is propagating along a ray trajectory, Σ (see Fig. 5). Denoting σ as the arc length along the ray trajectory, the ray local coordinates are defines by the unit-vectors $\hat{\mathbf{t}}$, $\hat{\mathbf{n}}$, $\hat{\mathbf{n}}_b=\hat{\mathbf{t}}\times\hat{\mathbf{n}}$, denoting the tangent, normal, and bi-normal of Σ at a point $\mathbf{r}_o(\sigma)$ on Σ, respectively. They are related by the Fernet equations[20]

$$\mathbf{r}_o'=\hat{\mathbf{t}},\quad \hat{\mathbf{t}}'=K\hat{\mathbf{n}},\quad \hat{\mathbf{n}}'=-K\hat{\mathbf{t}}+\kappa\hat{\mathbf{n}}_b,\quad \hat{\mathbf{n}}_b'=-\kappa\hat{\mathbf{n}}, \tag{44}$$

where the prime denotes a derivative with respect to σ, K is the curvature of Σ, and κ is its torsion. The ray coordinates are nonorthogonal for $\kappa\neq 0$. A locally orthogonal coordinate system along the ray may be obtain by transverse rotation of the unit-vectors[20] (see Fig. 5)

$$\begin{pmatrix} \hat{\mathbf{x}}_{b_1} \\ \hat{\mathbf{x}}_{b_2} \end{pmatrix} = \begin{pmatrix} \cos\theta & -\sin\theta \\ \sin\theta & \cos\theta \end{pmatrix} \begin{pmatrix} \hat{\mathbf{n}} \\ \hat{\mathbf{n}}_b \end{pmatrix}, \tag{45}$$

where $\theta(\sigma)$ satisfies

$$\theta'(\sigma) = \kappa(\sigma). \tag{46}$$

Points near the ray may now be expressed as

$$\mathbf{r} = \mathbf{r}_o(\sigma) + n\hat{\mathbf{n}}(\sigma) + n_b\hat{\mathbf{n}}_b(\sigma) = \mathbf{r}_o(\sigma) + x_{b_1}\hat{\mathbf{x}}_{b_1} + x_{b_2}\hat{\mathbf{x}}_{b_2}, \tag{47}$$

where the coordinate frame $(\sigma, x_{b_1}, x_{b_2})$ is locally orthogonal with $dr = \hat{\mathbf{t}}h_\sigma d\sigma + \hat{\mathbf{x}}_{b_1}dx_{b_1} + \hat{\mathbf{x}}_{b_2}dx_{b_2}$, with the Lamé coefficient

$$h_\sigma = 1 - K(\sigma)[x_1\cos\theta + x_2\sin\theta] = 1 - K(\sigma)n. \tag{48}$$

2. Asymptotic evaluation of the scattering propagator

The ray coordinate system may now be applied to the scattering propagators, $B_b^s(\mathbf{r}'; \overline{\mathbf{X}}^s)$. Each propagator arrives at the observation plane to point $\overline{\mathbf{x}}^s$ from a direction $\overline{\boldsymbol{\xi}}^s$; thus, we associate a ray coordinate system to each beam, so that ray parameters σ, x_{b_1} and x_{b_2} are all processing parameters $(\overline{\mathbf{X}}^s)$-dependent, and are denoted as $\sigma^s = \sigma(\overline{\mathbf{X}}^s)$, $\mathbf{x}_b^s = (x_{b_1}(\overline{\mathbf{X}}^s), x_{b_2}(\overline{\mathbf{X}}^s))$, etc. The inhomogeneous medium in the high frequency-localized beam excitation regime may be modelled by the wave speed along the excited ray and its second order transverse derivative matrix $\mathbf{V}_b^{(2)}(\sigma^s)$, whose (ij) elements are $\partial_{x_{b_i}}\partial_{x_{b_i}} v_b|_{\Sigma^s}$. Using the ray coordinate frame, the paraxially approximated scattering propagators may be evaluated in the high frequency regime, giving (see details in Appendix B)

$$B_b^s(\mathbf{r}^s; \overline{\mathbf{X}}^s) = \frac{i}{2k_o\overline{\zeta}^s}\sqrt{\frac{v_b(\sigma^s)}{v_o}\frac{\det\mathbf{Q}_b^s(0)}{\det\mathbf{Q}_b^s(\sigma^s)}}\exp[i\Phi_b^s(\mathbf{r}^s; \overline{\mathbf{X}}^s)], \tag{49}$$

with

$$\Phi_b^s(\mathbf{r}^s; \overline{\mathbf{X}}^s) = -\left[\int_0^{\sigma^s} d\sigma' k_b(\sigma')\right] + \frac{1}{2}k_b(\sigma^s)\mathbf{x}_b^s \quad \boldsymbol{\Gamma}_b^s(\sigma^s)\cdot\mathbf{x}_b^s, \tag{50}$$

where $k_b(\sigma^s) = \omega/v_b(\mathbf{r})|_{\mathbf{r}\in\Sigma^s}$ is the wave number along the excited ray Σ^s. The transverse matrix $\boldsymbol{\Gamma}^s(\sigma^s)$ is a complex symmetric 2×2 matrix with $\mathrm{Im}\,\boldsymbol{\Gamma}^s$ positive definite. One may calculate $\boldsymbol{\Gamma}^s$ by the standard procedure of solving the matrix Riccati equation, setting

$$\boldsymbol{\Gamma}_b^s(\sigma^s) = v_b(\sigma^s)\mathbf{P}_b(\sigma^s)\mathbf{Q}_b^{-1}(\sigma^s), \tag{51}$$

and solving, along Σ^s, the first order system of coupled differential equations

$$\mathbf{Q}_b'(\sigma^s) = v_b(\sigma^s)\mathbf{P}_b(\sigma^s), \quad \mathbf{P}_b'(\sigma^s) = -v_b(\sigma^s)^{-2}\mathbf{V}_b^{(2)}(\sigma^s)\mathbf{Q}_b(\sigma^s), \tag{52}$$

where the prime denotes a derivative with respect to the argument. Relation (52) is subject to the initial conditions

$$\mathbf{Q}_b(0) = \mathbf{I}, \quad \mathbf{P}_b(0) = v_o\boldsymbol{\Gamma}^s. \tag{53}$$

As in the special case of homogeneous background medium (i.e., the Born approximation) in (28), one can show that if $\boldsymbol{\Gamma}^s(0)$ is symmetric with $\mathrm{Im}\,\boldsymbol{\Gamma}^s(0)$ positive definite, then $\boldsymbol{\Gamma}^s(\sigma^s)$ has these

properties for all σ^s, and that $\mathbf{Q}(\sigma^s)\neq 0$ for all σ^s. Following the procedure in (32)–(35), one identifies $\mathrm{Re}\,\mathbf{\Gamma}^s(\sigma^s)$ and $\mathrm{Im}\,\mathbf{\Gamma}^s(\sigma^s)$ as the beam curvature and beam-amplitude matrices, respectively. Note that the special case of the Born approximation in (28), in which the background medium is homogeneous, may be obtained by substituting $v_b(\mathbf{r})=v_o$ into (49)–(53).

The scattering propagators, $B_b^s(\mathbf{r}';\overline{\mathbf{X}}^s)$, are backpropagating along the ray trajectory initiating from the scattered data plane in $z^s=0$, from a processing $\overline{\mathbf{x}}^s$-dependent point, in a processing $\overline{\boldsymbol{\xi}}^s$-dependent direction. The propagator exhibits a Gaussian decay normal to the ray trajectory, i.e., in $\mathbf{x}_b^s$.

3. Asymptotic evaluation of the incident propagators

For the case of the incident propagators, $B_b^i(\mathbf{r}';\overline{\mathbf{X}}^i)$, in (18), each propagator emanates from point $\overline{\mathbf{x}}'$ on the initial distribution plane, in a direction $\overline{\boldsymbol{\xi}}^i$ (see Fig. 3); thus, the ray coordinates associated with each processed beam are denoted accordingly as $\sigma^i=\sigma(\overline{\mathbf{X}}^i)$, etc. As in (49), the inhomogeneous medium may be modeled by the wave number along the excited ray, $k_b(\sigma^i)$, and its second order transverse derivative matrix $\mathbf{V}_b^{(2)}(\sigma^i)$ along the beam-axis. Using the ray coordinate frame, the paraxially approximated scattering propagators may be evaluated in the high frequency regime in a manner similar to (49), giving

$$B_b^i(\mathbf{r};\overline{\mathbf{X}}^i)=\sqrt{\frac{v_b(\sigma^i)}{v_o}\frac{\det\mathbf{Q}_b^i(0)}{\det\mathbf{Q}_b^i(\sigma^i)}}\exp[i\Phi_b^i(\mathbf{r};\overline{\mathbf{X}}^i)] \tag{54}$$

with

$$\Phi_b^i(\mathbf{r};\overline{\mathbf{X}}^i)=\left[\int_0^{\sigma^i}d\sigma' k_b(\sigma')\right]+\frac{1}{2}k_b(\sigma^i)\mathbf{x}_b^i\quad\mathbf{\Gamma}_b^i(\sigma^i)\cdot\mathbf{x}_b^i, \tag{55}$$

where the matrix $\mathbf{\Gamma}_b^i(\sigma^i)$ is found by solving (52) along the incident beam-axis $\sigma^i\in\Sigma^i$ with the initial conditions $\mathbf{Q}_b(0)=\mathbf{I}$ and $\mathbf{P}_b(0)=v_o\mathbf{\Gamma}^i$.

4. PS2PS mapping

Next, we consider the scattering cell under Gaussian windows processing. By inserting $B_b^s(\mathbf{r}';\overline{\mathbf{X}}^s)$ in (49) with $B_b^i(\mathbf{r}';\overline{\mathbf{X}}^i)$ in (54) into (22), we obtain the asymptotic expression for the scattering cell

$$\Lambda_b(\mathbf{r}';\overline{\mathbf{X}}^i,\overline{\mathbf{X}}^s)=\frac{ik_o}{8\pi^2\overline{\zeta}^sN^i}\sqrt{\frac{v_b(\sigma^s)v_b(\sigma^i)/v_o^2}{\det\mathbf{Q}_b^s(\sigma^s)\det\mathbf{Q}_b^i(\sigma^i)}}\exp\{i[\Phi_b^s(\mathbf{r}^s;\overline{\mathbf{X}}^s)+\Phi_b^i(\mathbf{r};\overline{\mathbf{X}}^i)]\}, \tag{56}$$

where Φ_b^s and Φ_b^i are given in (50) and (55), respectively. Relation (56) implies the following: The local scattering cell exhibits Gaussian decay normal to both the incident and scattering ray trajectories (i.e., in $\mathbf{x}_b^i$ and $\mathbf{x}_b^s$). Thus, the window center is located at the intersection of the incident spectral beam $B_b^i(\mathbf{r}';\overline{\mathbf{X}}^i)$ and the scattered beam propagator $B_b^s(\mathbf{r}';\overline{\mathbf{X}}^s)$ axes. Therefore, the location of the scattering cell is resolved by the PS processing parameters $\overline{\mathbf{X}}^s$ and $\overline{\mathbf{X}}^i$, which determine, via (30), the PS propagators ray trajectories (see Fig. 3).

The localization in the object domain as determined by $\Lambda_b(\mathbf{r}';\overline{\mathbf{X}}^i,\overline{\mathbf{X}}^s)$ may be interpreted by using fundamental wave physics. Consider an incident propagator emanating from $z=0$ plane from point $\overline{\mathbf{x}}'$ at angle $\overline{\theta}^i$ along ray Σ^i, arriving at the $z^s=0$ scattering plane at point $\overline{\mathbf{x}}^s$ at angle $\overline{\theta}^s$. In this case, the scattering propagator, $B_b^s(\mathbf{r};\overline{\mathbf{X}}^s)$, corresponding to $\overline{\mathbf{x}}^s$ and $\overline{\theta}^s$, backpropagates along the same ray trajectory $\Sigma^s=\Sigma^i$, and the corresponding scattering cell exhibits Gaussian decay *only* in the transverse coordinates $(\mathbf{x}_{b_1},\mathbf{x}_{b_2})$ and not along the (shared) beam-axis. Therefore, the integration domain in (21) is local *only normal to* Σ^i, which indicates the stationary

contribution to PS spectral distribution at that particular $\overline{\mathbf{X}}^s$ in accord with the Fermat principle. Furthermore, the phase accumulation along Σ^i, $2\int_0^{\sigma^i} d\sigma' k_b(\sigma')$, when introduced into (21), acts as a ''scaled Fourier transform'' operating along the ray trajectory; thus, large contributions to Ψ_b in (21) arise from medium variations *along* Σ in accord with fundamental 1D wave physics.

V. CONCLUDING REMARKS

Inhomogeneous medium Green's function in the phase-space domain were presented, linking the phase-space spectral distributions of the field scattered by a high contrast object to a genetic time-harmonic incident field. Two forms of phase-space Green's function were presented: (a) A *configuration-space to phase-space* Green's function that links induced sources in the object domain to phase-space distributions of the scattered field is obtained by applying PS transform to the scattered field over planar surfaces; and (b) a *phase-space to phase-space* Green's function, which directly links incident- to scattered-phase-space distribution, obtained by applying the PS transform to *both* incident and scattered field distributions, s. The scattering mechanism has been described in terms of local samplings of the object function which are localized in the object domain according to the scattered- and incidence-processing parameters. The special case of Gaussian windows has been considered and asymptotic expressions for the PS Green's functions and scattering cells have been derived for both the Born approximated- and the generic-inhomogeneous medium profiles. The wave phenomenology associated with the PS Green's functions and the scattering mechanism have also been explored.

Equations (20)–(22) establish the building blocks for an *inverse scattering* procedure in which the strong scatterer is found via iterative algorithm where at the nth iteration, the background $v_b(\mathbf{r})=v_n(\mathbf{r})$ is known, and the sampling operation in (20) is inverted to evaluate $O(\mathbf{r})$, from which the next v_{n+1} is found. This operation may be carried out for large scatterers since it can be shown that under appropriate illuminating conditions, the operation in (20) may be reduced to 1D samplings along the (synthesized) scattered ray trajectories.

ACKNOWLEDGMENT

This research was supported by a grant from the G.I.F., The German–Israeli Foundation for Scientific Research and Development.

APPENDIX A: OPERATOR REPRESENTATION OF CS2PS GREEN'S FUNCTION

In order to establish the scattering propagators in (11) as Green's functions, an operator equation associated with the CS2PS is derived hereby. We define the Helmholtz operator $(L_1u)(\mathbf{r})$

$$(L_1u)(\mathbf{r})\equiv[\nabla^2+k_b^2(\mathbf{r})]u(\mathbf{r}), \tag{A1}$$

and the inverse-PS operator $(L_2U)(\overline{\mathbf{X}})$

$$(L_2U)(\overline{\mathbf{X}})\equiv\left(\frac{k_o}{2\pi N^s}\right)^2\int d^4\overline{X}^s \;\; U(\overline{\mathbf{X}},z^s) \;\; W^s(\mathbf{x}^s;\mathbf{X}^s), \tag{A2}$$

where $U(\overline{\mathbf{X}},z^s)$ are PS distributions over planar surfaces of constant z^s. Next, we define the cascade operator $(LU)(\overline{\mathbf{X}})=[L_1(L_2U)(\overline{\mathbf{X}})][\mathbf{r}]$. Using (9), in (1), we identify the operator equation

$$(LU^s)(\overline{\mathbf{X}}^s)=-f(\mathbf{r}), \quad f(\mathbf{r})=k_o^2O(\mathbf{r})u(\mathbf{r}). \tag{A3}$$

The Green's function, B_b^s, associated with the operator Eq. (A3) is obtained by solving

$$(LB_b^s)(\overline{\mathbf{X}}^s) = -\delta(\mathbf{r}-\mathbf{r}') \tag{A4}$$

and the resolvent operator of L, $U^s=(L^{-1}f)(\mathbf{r})$ takes the form in (10), thereby identifying B_b^s in (11) as a Green's function. Furthermore, by substituting (11) into (A3) and inverting the order of integration, one finds that the PS scattering propagators satisfy definition (A4).

APPENDIX B: EVALUATION OF EQ. (49)

In order to establish Eq. (49), we note that generic solution for beam-type wave objects propagating in the background medium $v_b(\mathbf{r})$, along the ray Σ^s, is given by[3,14,19]

$$B_b^s(\mathbf{r}) = A\sqrt{\frac{v_b(\sigma^s)}{v_o}\frac{\det\mathbf{Q}_b(0)}{\det\mathbf{Q}_b(\sigma^s)}}\exp[i\Phi_b(\mathbf{r})], \tag{B1}$$

where A is a constant, and the phase

$$\Phi_b(\mathbf{r}) = \pm\left[\int_0^{\sigma^s} d\sigma' k_b(\sigma')\right] + \frac{1}{2}k_b(\sigma^s)\mathbf{x}_b \quad \mathbf{\Gamma}_b(\sigma^s)\cdot\mathbf{x}_b\,. \tag{B2}$$

Since, according to (11), the scattering propagator $B_b^s(\mathbf{r}';\overline{\mathbf{X}}^s)$ satisfies wave equation (1) with $v(\mathbf{r})=v_b(\mathbf{r})$, we seek for solutions in the form of (B1). Under the paraxial approximation, the initial distribution of the scattering propagator over the $z^s=0$ plane may be replaced by the initial parameter matrix (see discussion following (42))

$$\mathbf{\Gamma}^s_{\text{parax}} = \begin{bmatrix} \Gamma^{s*}/\overline{\zeta^s}^2 & 0 \\ 0 & \Gamma^{s*} \end{bmatrix}, \tag{B3}$$

over the $z_b^s=0$ plane. Note that the projected initial paraxial distribution, which was originally obtained for homogeneous medium, may serve for inhomogeneous propagation as well, as long as the initial plane is embedded in an homogeneous medium, since in the high-frequency limit Bremmer-type reflections are negligible, and the beam-type field is forward propagating along the ray trajectories.[3,14] Therefore, we may use the homogeneous background asymptotic field in (28) with the above-mentioned initial distribution in the general solution (B1) yielding (49). Note that solution (49) satisfies the radiation condition of sources in the $z^s<0$ as exhibited by the propagation phase accumulation of $-\int_0^{\sigma^s} d\sigma' k_b(\sigma')$ for $\sigma^s<0$ (see also Fig. 4).

[1] L. B. Felsen and N. Marcuvitz, *Radiation and Scattering of Waves* (IEEE, New Jersey, 1994).
[2] L. B. Felsen, J. Opt. Soc. Am. A **2**, 954 (1985).
[3] M. M. Popov, V. Červeny, and I. Pšenčík, Geophys. J. R. Astron. Soc. **70**, 109 (1982).
[4] E. Heyman, Wave Motion **11**, 337 (1989).
[5] M. J. Bastiaans, Optik (Stuttgart) **57**, 95 (1980).
[6] P. D. Einziger, S. Raz, and M. Shapira, J. Opt. Soc. Am. A **3**, 508 (1986).
[7] J. J. Maciel and L. B. Felsen, IEEE Trans. Antennas Propag. **37**, 884 (1989).
[8] B. Z. Steinberg, E. Heyman, and L. B. Felsen, J. Opt. Soc. Am. A **8**, 41 (1991).
[9] A. Dendane and J. M. Arnold, IEE Proc., Part H: Microwaves, Antennas Propag. **141**, 216 (1994).
[10] J. M. Arnold, J. Opt. Soc. Am. A **12**, 111 (1995).
[11] T. Melamed, J. Electromagn. Waves Appl. **11**, 739 (1997).
[12] J. M. Arnold and L. B. Felsen, Opt. Express **10**, 716 (2002).
[13] D. Lugara, C. Letrou, A. Shlivinski, E. Heyman, and A. Boag, Radio Sci. **38**, 8026 (2003).
[14] E. Heyman, IEEE Trans. Antennas Propag. **42**, 311 (1994).
[15] T. Melamed, E. Heyman, and L. B. Felsen, IEEE Trans. Antennas Propag. **47**, 1208 (1999).
[16] T. Melamed, E. Heyman, and L. B. Felsen, IEEE Trans. Antennas Propag. **47**, 1218 (1999).
[17] B. Z. Steinberg, E. Heyman, and L. B. Felsen, J. Opt. Soc. Am. A **8**, 943 (1991).
[18] E. Heyman and T. Melamed, IEEE Trans. Antennas Propag. **42**, 518 (1994).
[19] E. Heyman and L. B. Felsen, J. Opt. Soc. Am. A **18**, 1588 (2001).
[20] V. M. Babič and V. S. Buldyrev, *Short-Wavelength Diffraction Theory: Asymptotic Methods* (Springer-Verlag, Berlin, 1991).